

A New Algorithm for Improved Blind Detection of Polar Coded PDCCH in 5G New Radio

Amin Jalali, *Student Member, IEEE*, and Zhi Ding, *Fellow, IEEE*

Abstract—In recent release of the new cellular standard known as 5G New Radio (5G-NR), the physical downlink control channel (PDCCH) has adopted polar codes for error protection. Similar to 4G-LTE, each active user equipment (UE) must blindly detect its own PDCCH in the downlink search space. This work investigates new ways to improve the accuracy of PDCCH blind detection in 5G-NR. We develop a novel design of joint detection and decoding receiver for 5G multiple-input multiple-output (MIMO) transceivers. We aim to achieve robustness against practical obstacles including channel state information (CSI) errors, noise, co-channel interferences, and pilot contamination. To optimize the overall receiver performance in PDCCH blind detection, we incorporate the polar code information during the signal detection stage by relaxing and transforming the Galois field code constraints into the complex signal field. Specifically, we develop a novel joint linear programming (LP) formulation that takes into consideration the transformed polar code constraints. Our proposed joint LP formulation can also be integrated with polar decoders to deliver superior receiver performance at low cost. We further introduce a metric that can be used to eliminate most of wrong PDCCH candidates to improve the computational efficiency of PDCCH blind detection for 5G-NR.

Index Terms—5G, PDCCH, polar codes, linear programming, joint detection-decoding, blind detection

I. INTRODUCTION

IN modern mobile wireless communication standards such as the 3GPP LTE/LTE-Advanced [1] and the 3GPP NR [2], active user-equipment (UE) devices must obtain crucial control messages known as downlink control information (DCI) from the serving gNB. It is highly critical for the UE to correctly receive its DCI that are placed in the PDCCH search space since receiving data which will be sent in physical downlink shared channel (PDSCH) depends on it. Since a UE does not know the location of its DCI in the search space, it must perform so-called blind detection by attempting to decode a set of possible DCI candidates. According to the 3GPP standards [1] [2], the number of such candidates may even exceed forty. Thus, using a complex decoder for error-correcting codes on all candidates is costly in terms of computation, latency, and power consumption. Therefore, it is of practical importance to investigate means for improving both the detection performance and the computation efficiency.

In the 4G cellular communication standards by the 3GPP, the control message (DCI) is encoded with convolutional codes

for which blind detection algorithms have been designed [3]–[6]. Other blind-detection algorithms for low-density parity check (LDPC) codes [7] and Bose-Chaudhuri-Hocquenghem (BCH) [8] codes have also been proposed. However, in the 5G cellular communication standard (5G), a more interesting class of forward error correcting (FEC) codes known as polar codes are adopted for error protection of PDCCH. Polar codes, discovered by Arkan in 2008, have been shown to achieve channel capacity on binary-input discrete memoryless channels (BDMCs) without high encoding and decoding complexities [9], [10]. Many investigative works on polar codes have appeared, including their construction and use under additive white Gaussian noise (AWGN) channels [10]–[12] and fading channels [13]. Successful and popular decoder algorithms include successive cancellation (SC) decoding [9] and successive cancellation list (SCL) decoding introduced in [14]. Effective algorithms for the blind detection of polar coded DCI in 5G cellular networks remain an open problem. Accurate detection of polar coded DCI by the UE is of critical importance to the success of cellular communications. This work focuses the development of reliable and low complexity blind detection of DCI signals by jointly exploiting the antenna diversity and polar code constraints to develop a novel and integrative receiver algorithm.

In most modern wireless communication systems, multiple-input multiple-output (MIMO) transceivers have been widely adopted owing to their ability to achieve high spectral efficiency. As a result, robust and efficient receivers for MIMO wireless systems have been widely investigated in the literature. It is well known that maximum likelihood detector (MLD) can optimally minimize the probability of detection error. Well known MLD algorithms for MIMO systems include the sphere decoding [15] and a V-BLAST detection [16]. Ideally, optimum receiver performance can be accomplished by applying the principle of maximum likelihood detection under the FEC codeword constraints to reject that symbol sequences that belong to invalid FEC codewords. However, for most FEC codes that are not very short, joint maximum likelihood detection and decoding (MLDD) can be extraordinarily complex and costly to implement. As a result, most practical MIMO receivers apply MIMO detection followed by FEC decoding separately. The lack of joint MLDD is attributed to the NP-hard high complexity of incorporating Galois field FEC constraints into maximum likelihood symbol detection criteria that operate strictly in Euclidean (real or complex) field. To overcome the difficulty posed by the conflicting fields of detection versus decoding, existing joint MIMO detection and FEC decoding receivers typically utilize the exchange of

The authors are with the Department of Electrical and Computer Engineering, University of California at Davis, Davis, CA 95616 USA (e-mail: amjal@ucdavis.edu; zding@ucdavis.edu).

This work was presented in part at the 2018 IEEE International Symposium on Information Theory in Vail, Colorado, USA

This material is based on works supported by the National Science Foundation under Grants 1700762 and 1711823

soft information between soft decoder and detector to form a turbo receiver [17]–[21].

Recently, a new type of receiver based on joint detection and decoding has been proposed [22], [23]. Transforming the Galois field code constraints into a set of linear inequality constraints in the Euclidean field, a joint linear programming (LP) receiver can leverage the constraints imposed by modulated data symbols, training symbols, noise subspace, and the LPDC code to achieve improved performance. The concept of joint detection-decoding has been applied in massive MIMO systems to combat pilot contamination [24] [25] and also used to tackle channel uncertainties such as partial channel information [26], [27] or imperfect channel estimation [28].

In this work, we study how the joint detection-decoding principle based on integrated constraints in Euclidean field can improve the receiver performance in the practical PDCCH detection for 5G cellular receivers. Our chief objective is to enable UE receivers to eliminate false PDCCH candidates during the signal detection stage and to reduce receiver delay and energy consumption. We also aim to develop UE receivers to be reliable and robust against practical non-idealities including CSI errors, noises, co-channel interferences, and pilot contamination. To achieve our goals, we formulate an LP optimization problem for the joint MIMO detector that incorporates relaxed polytope polar code constraints. This relaxed polytopes, proposed in [29] are constructed according to the factor graph representation of polar codes and achieve the ML-certificate property. Furthermore, we take advantage of these code constraints in the LP formulation in order to define a metric that we call *fractional metric*. We show that this metric is capable of identifying the polar codewords in detection stage. Based on the fractional metric, we propose a new algorithm to improve the blind detection of DCI by eliminating all but one of the candidates for decoding. Substantially reducing the number of decoding steps, our proposed blind detection algorithm is capable of saving receiver latency and power consumption substantially while maintaining a very low probability of missed detection in the search space.

We note that blind detection of polar coded messages has been investigated recently in [30], [31] as well. In particular, the authors of [31] proposed a different detection metric for identifying whether a received block may be a candidate block encoded by a particular polar code. The authors of [30] developed a blind detection scheme that requires transmitting the radio network temporary identifier (RNTI) on some of the frozen bits of the polar code before letting the decoder to eliminate a subset of candidates in the search space. On the other hand, our proposed blind detection algorithm utilizes the code constraints to form a novel integrative detector. Since the metric that we propose in this paper is readily accessible at the detector, it can be easily integrated with the existing schemes of [30], [31].

In this paper, we first introduce the problem of DCI blind detection in PDCCH search space of 5G cellular networks in Section II. We shall introduce the basic principles of polar codes. In Section III, we present a problem formulation of FEC coded MIMO detector as linear program by incorporating the polar code constraints based on the approach in [29] to

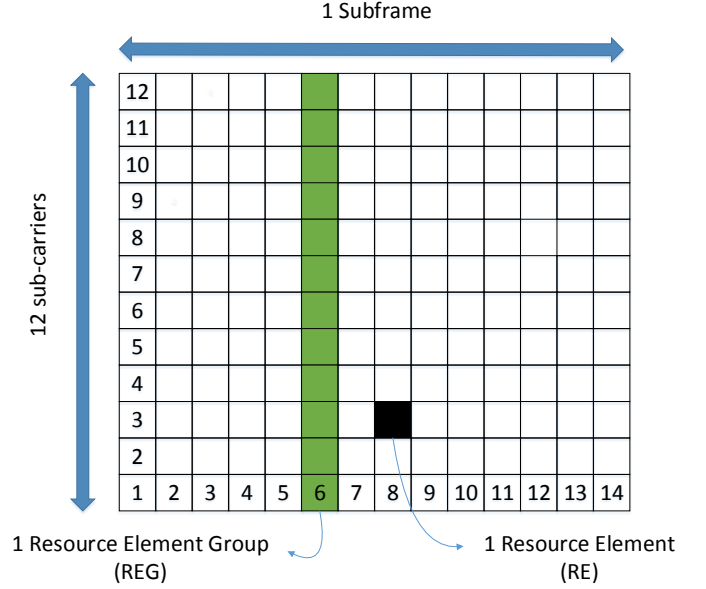


Fig. 1. 5G/NR frame structure terminology, Normal CP, $\mu = 0$ (15KHz subcarrier spacing)

develop a novel joint LP receiver. This new joint receiver effectively exploits the rich and important diversity of FEC code constraints and is robust against practical non-idealities including CSI errors, noises, co-channel interferences, and pilot contamination. Our proposed joint LP receiver can also be integrated with popular polar decoders such as SC and SCL decoders for reduced complexity implementation. In Section IV, we propose a metric obtained in solving LP optimization problem and present an algorithm using this metric to identify the right DCI candidate in the search space that contain the UE control message. We present simulation results in Section V to illustrate the efficacy of the proposed receiver design both in terms of BER/BLER and also its capability to improve blind detection process, before concluding this paper in section VI.

II. SYSTEM MODEL

A. 5G Downlink Physical Parameters

As described in 3GPP new radio (NR) standard [2], the time intervals are expressed with a basic time unit $T_c = 1/1966080000$ seconds. Similar to 4G-LTE, each radio frame has a length of 10 ms and is equally divided into ten subframes of 1 ms in duration; however, in NR, OFDM subcarrier spacing is scalable based on the numerology (μ). For $\mu = 0$ and normal cyclic prefix case, each subframe consists of 14 OFDM symbols, as illustrated in Fig. 1.

A resource element (RE) is the smallest unit of the resource grid made up of one OFDM sub-carrier for one OFDM symbol interval. A physical resource block (RB) is the smallest unit of resources that can be allocated to a user. Without loss of generality, we can consider numerology $\mu = 0$ [2], for which the subcarrier spacing is 15 kHz. The resource block is 180 kHz wide in frequency. A resource element group (REG) is made up of 12 resource elements in frequency domain and one OFDM symbol in time domain. Moreover, multiple

continuous REGs constitute a control channel element (CCE) that is used to carry downlink control information (DCI). Aggregation level indicates how many CCEs are allocated for PDCCH, depending on the DCI size. Based on NR standard [2], aggregation level can be 1/2/4/8/16. Control resource set (CORESET), consists of multiples of 12 REs in frequency domain, across 1/2/3 OFDM symbols in time domain. CORESET is equivalent to the control region in LTE subframe [2].

The DCI uses QPSK modulation and carries information about downlink shared channel (DL-SCH) resource allocation. gNB schedules the downlink shared channel (DL-SCH) resource blocks for different users through the DCI. DCI also contains the information regarding DL-SCH hybrid automatic repeat request (HARQ). Clearly, it is vital for each UE to correctly decode its DCI to receive actual downlink data messages.

B. Blind Detection

UE needs to calculate the number of available CCEs used for downlink control information and index them. This depends on depend on CORESET, bandwidth of the system and number of antenna ports present which in turn will affect the number of reference signals present. To calculate the number of CCEs available for PDCCH, UE first needs to calculate the number of REs used for PDCCH by subtracting REs used for reference symbols, PCFICH, and PHICH, respectively, from the total REs that are allocated for control region. Suppose 3 first symbols are allocated for control region while the bandwidth is 10 Mhz to allow 50 RBs. Therefore

$$\text{Total REs} = 3 \times 12 \times 50 = 1800\text{REs}$$

Then we calculate number of REs for PDCCH by

$$\begin{aligned} \text{REs for PDCCH} = & \text{Total REs} - \\ & \text{Number of REs used for reference signals} - \\ & \text{Number of REs used in PHICH} - \\ & \text{Number of REs used in PCFICH} \end{aligned}$$

$$\text{CCEs available for PDCCH} = \frac{\text{REs for PDCCH}}{\text{Number of REG per CCE} \times 12}$$

Next, each active and searching UE shall group the remaining REs into CCEs and index them. The first 16 CCEs belong to common search space (CSS) in which control information is relevant to all the receiving UEs. If there are more than 16 CCEs available, the remainder would be used to send UE-specific control information that is only decodable for a particular UE. This particular space is called UE specific search space (UESS).

Suppose, there are total number of 40 CCEs that gNB can send DCI for a particular UE. If that particular UE does not know at which index it needs to start scanning and also how many consecutive CCEs consisting its DCI (aggregation level), then it would face overwhelming number of candidates to check. To limit the search space so as to save energy and computation cost, the gNB fixes some CCE indices for

TABLE I
NUMBER OF PDCCH CANDIDATES FOR DIFFERENT AGGREGATION LEVELS AND SEARCH SPACE TYPE

search type	space	aggregation level	size (in CCEs)	number of PDCCH candidates
UESS		1	6	6
		2	12	6
		4	8	2
		8	16	2
CSS		4	16	4
		8	16	2

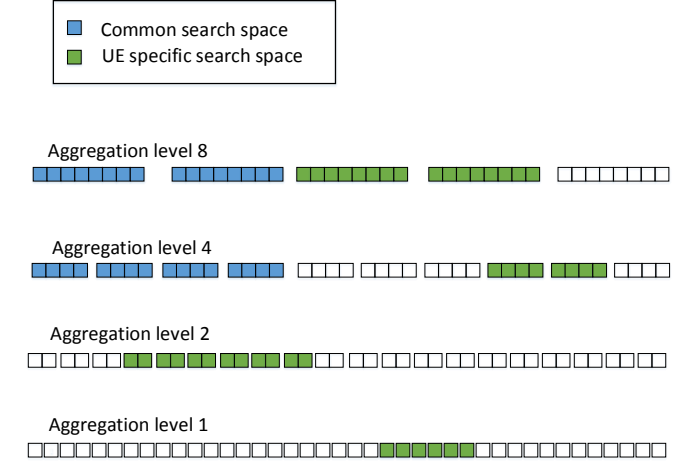


Fig. 2. Common and UE specific search space for each aggregation level

a particular UE. This means that the UE knows, for each aggregation level, what CCE indices to start looking for among all indices, based on a formula related to its RNTI and the subframe number which are known to both the UE and serving gNB.

In Table I, the number of CCE indices and PDCCH candidates searched by a UE in a subframe for each search space has been mentioned for LTE standard [1]. Figure 2 is based on Table I and graphically shows the hypothetical PDCCH indices to scan for each aggregation level, from all the potential indices.

For instance, for CSS with 16 CCEs, aggregation level can be either 4 or 8. There are 2 possible DCI formats in CSS. Therefore, in case of aggregation level 4, UE needs to consider CCE index 0, 4, 8 and 12. For aggregation level 8, it needs to consider CCE index 0 and 8. Hence, in this case the number of PDCCH candidates can be calculated as:

$$\begin{aligned} & (4[\text{in aggr. level 4}] + 2[\text{in aggr. level 8}]) \\ & \times (2 [\text{DCI formats in CSS}]) = 12. \end{aligned}$$

Therefore, UE needs to calculate the CCE indices possible for each aggregation level for both CSS and UESS, to get the PDCCH candidates. After decoding each PDCCH candidate, the UE shall use the 16-bit cyclic redundancy check (CRC) code appended to the DCI payload in order to verify whether the candidate is the correct one for the UE. The gNB masks the CRC using the UE specific RNTI as a distinct identifier. The

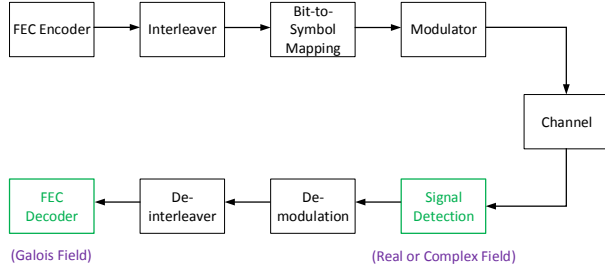


Fig. 3. Polar-coded MIMO system

UE validates the decoded candidate by checking the unmasked CRC code. If a PDCCH candidate passes the CRC after RNTI unmasking, the UE shall claim the PDCCH candidate as its own correctly decoded DCI. This necessary UE process in cellular communications is called blind detection or blind decoding in the 3GPP standards of 4G-LTE and 5G-NR.

Blind detection saves downlink bandwidth since no additional signaling is needed to indicate to the UE the location of its DCI. By letting the UE detect its DCI in the search space, blind detection trades computation for bandwidth. There naturally exists accompanied latency and energy consumption, particularly when a computationally expensive channel decoder is used. Thus, it is highly desirable to improve the performance of the detection so as to reduce the set of candidates that are sent to the UE decoder. Our novel proposal of a joint DCI detector is capable of generating a metric that helps the UE to considerably reduce the number of such search candidates.

C. Polar Code for Error Protection

Figure 3 illustrates a generic polar-coded MIMO transmission system in which information bits are first encoded with polar encoder as FEC (forward error correction) codewords before being mapped into QAM data symbols of constellation \tilde{Q} . Note that PDCCH uses QPSK modulation for data symbols. The MIMO receiver aims to recover the source bits despite channel distortions, interferences, and channel noises. Our goal is to design a joint detector that incorporates the polar code information that is in Galois field in MIMO signal detection for improved performance.

Briefly, a polar code of rate $R = K/N$ is specified by (N, K, \mathcal{I}^c) , where $N = 2^n$ is the codeword length and K is the number of information bits in a codeword. Let $\mathcal{I} \subseteq \{1, \dots, N\}$ denote the set of indices of the information bits whose complement set \mathcal{I}^c denotes the set of frozen (non-information bearing) bits. Let $\mathbf{u} = [u_1, u_2, \dots, u_N]$ denote the binary information vector and let $\mathbf{b} = [b_1, b_2, \dots, b_N]$ denote the binary codeword vector. There is a 1-1 mapping between \mathbf{u} and \mathbf{b} defined by $\mathbf{b} = \mathbf{u}\mathbf{G}_N$ in which \mathbf{G}_N is the generator matrix of the polar code. Note that \mathbf{G}_N is defined through $\mathbf{G}_N = \mathbf{B}_N\mathbf{F}^{\otimes n}$, where \mathbf{B}_N is a bit reversal operator defined in [9], and $\mathbf{F}^{\otimes n}$ denotes n -fold Kronecker power of polarization kernel

$$\mathbf{F} = \begin{bmatrix} 1 & 0 \\ 1 & 1 \end{bmatrix} \quad (1)$$

Using the concept of channel polarization, N identical realization of the channel can be transformed into N parallel virtual bit-channels, which become polarized as either extremely noisy or completely error-free as N tends to infinity. Consequently, the crucial step in constructing polar codes is to sort the virtual bit-channels based on their capacity and to select the K most reliable ones out of N bit-channels to carry information bits. The remaining $N - K$ bit-channels will carry the frozen bits (set to known values). As shown in [9], the fraction of reliable virtual channels among all the virtual channels is K/N , which approaches asymptotically to the channel capacity for large N . As a result, polar codes can achieve channel capacity for asymptotically long the codeword length $N \rightarrow \infty$ in B-DMCs.

D. Channel Model

Without loss of generality, we consider an MIMO system with n transmit antennas at the BS and m receive antenna at each UE.

For length N polar codeword and Q -ary QAM constellation, we can transmit one codeword via $K_0 = N/Q$ data symbols. For each subcarrier index k we can define complex QAM symbol $\tilde{x}_{i,k} \in \tilde{Q}$ and QAM vector $\tilde{\mathbf{x}}[k] = [\tilde{x}_{1,k}, \dots, \tilde{x}_{n,k}]^T$ as the transmission signal vector. Let each received symbol be $\tilde{y}_{i,k} \in \mathbb{C}$ and the received signal vector be $\tilde{\mathbf{y}}[k] = [\tilde{y}_{1,k}, \dots, \tilde{y}_{m,k}]^T$. By defining $\tilde{\mathbf{H}}[k] \in \mathbb{C}^{m \times n}$ as the linear $m \times n$ MIMO channel matrix for a flat fading wireless channel of each UE, we can write the received signal vector as

$$\tilde{\mathbf{y}}[k] = \tilde{\mathbf{H}}[k]\tilde{\mathbf{x}}[k] + \tilde{\mathbf{n}}[k], \quad k = 1, \dots, K_0 \quad (2)$$

in which $\tilde{\mathbf{n}}[k] = [\tilde{n}_{1,k}, \dots, \tilde{n}_{m,k}]^T \in \mathbb{C}^m$ is the additive white Gaussian noise (AWGN) vector whose elements are i.i.d. complex random variables and $\tilde{n}_{i,k} \sim \mathcal{CN}(0, \sigma_n^2)$. Note that the elements of $\tilde{\mathbf{H}}[k]$ are typically unknown and are estimated by relying on pilot symbols. Moreover, without loss of generality, we assume that the channel for each two REs are independent and not the same.

E. Maximum Likelihood Receiver

Since the multi-carrier MIMO channels are known or estimated at the receiver, the optimal maximum likelihood detector (MLD) that minimizes the probability of error for each transmission k can solve the problem

$$\min_{\tilde{\mathbf{x}} \in \tilde{Q}^{K_0}} \sum_{k=1}^{K_0} \|\tilde{\mathbf{y}}[k] - \tilde{\mathbf{H}}[k]\tilde{\mathbf{x}}[k]\|_2^2 \quad (3)$$

It should be noted that this MLD receiver does not yet take into consideration the fact that a data symbol vector $\tilde{\mathbf{x}}$ must be modulated by bits in an FEC codeword. In other words, only valid FEC codewords should be considered in the MLD receiver. Eliminating invalid codewords in MLD would have taken into consideration of the Galois field code constraints within the detection stage to minimize the probability of producing wrong symbol sequence by the detector to achieve better performance. Codeword constraints are even

more critical when our estimate of the channel matrix $\tilde{\mathbf{H}}$ is itself inaccurate.

We can denote the bits in each FEC codeword of length N as $\mathbf{b} = [b_1 \ b_2 \ \dots \ b_N]$ which should span K_0 data vectors, i.e.,

$$\tilde{\mathcal{M}}(\mathbf{b}) = \{\tilde{\mathbf{x}}[1], \tilde{\mathbf{x}}[2], \dots, \tilde{\mathbf{x}}[K_0]\}$$

where $\tilde{\mathcal{M}}(\cdot)$ denotes the mapping of FEC bits to data symbols for transmission. Consequently, the optimum receiver can be written as

$$\min_{\mathbf{b}} \sum_{k=1}^{K_0} \|\tilde{\mathbf{y}}[k] - \tilde{\mathbf{H}}\tilde{\mathbf{x}}[k]\|_2^2 \quad (4a)$$

$$\tilde{\mathcal{M}}(\mathbf{b}) = \{\tilde{\mathbf{x}}[1], \tilde{\mathbf{x}}[2], \dots, \tilde{\mathbf{x}}[K_0]\} \quad (4b)$$

$$\mathbf{b} \in \mathcal{F} \quad (4c)$$

where \mathcal{F} denotes the set of all valid FEC codewords of length N .

This exact ML optimization problem is a non-convex optimization problem and is highly complex to solve even for moderately long codeword because it requires exhaustive search over all valid set of symbols $\tilde{\mathcal{M}}(\mathbf{b}) = \{\tilde{\mathbf{x}}[1], \tilde{\mathbf{x}}[2], \dots, \tilde{\mathbf{x}}[K_0]\}$ that satisfy the coding constraints. Such problem is an NP-hard problem whose complexity grows exponentially with n . Furthermore, the constraint that requires $\mathbf{b} \in \mathcal{F}$, is defined in Galois field and obviously is a non-convex constraint when considering the Euclidean-field optimization in Eqs. (4).

In the next section we show how to modify the cost function and the constraints in (4) into an LP optimization problem to derive a unified joint receiver.

III. LP RECEIVER WITH POLAR CODING CONSTRAINTS

A. Redefining the Objective Function

To formulate a joint LP receiver, our first step is to modify the objective function by changing the l_2 norm in (3) to l_1 norm metric. The l_1 norm as an optimization metric has been applied in data analysis and parameter estimation because it is robust to impulsive noises and other man-made radio interferences [32]. To simplify the l_1 notation, we shall reformulate the problem in real field.

We assume that our modulation symbols $\tilde{x}_{i,k}$ are from a constellation \tilde{Q} that can be split into real and imaginary parts such as the most common quadrature amplitude constellation (QAM). More specifically, the real part $\text{Re}\{\tilde{x}_{i,k}\}$ and its imaginary part $\text{Im}\{\tilde{x}_{i,k}\}$ form the coordinate of a symbol in the same constellation \tilde{Q} . Consequently, we can transform our system from complex field to real field by defining

$$\mathbf{y}[k] = \begin{bmatrix} \text{Re}\{\tilde{\mathbf{y}}[k]\} \\ \text{Im}\{\tilde{\mathbf{y}}[k]\} \end{bmatrix}, \mathbf{x}[k] = \begin{bmatrix} \text{Re}\{\tilde{\mathbf{x}}[k]\} \\ \text{Im}\{\tilde{\mathbf{x}}[k]\} \end{bmatrix}, \mathbf{n}[k] = \begin{bmatrix} \text{Re}\{\tilde{\mathbf{n}}[k]\} \\ \text{Im}\{\tilde{\mathbf{n}}[k]\} \end{bmatrix} \quad (5)$$

and

$$\mathbf{H}[k] = \begin{bmatrix} \text{Re}\{\tilde{\mathbf{H}}[k]\} & -\text{Im}\{\tilde{\mathbf{H}}[k]\} \\ \text{Im}\{\tilde{\mathbf{H}}[k]\} & \text{Re}\{\tilde{\mathbf{H}}[k]\} \end{bmatrix} \quad (6)$$

Given the new notations in the real Euclidean field, we can write our system equation between the channel input $\mathbf{x}[k]$ and the channel output $\mathbf{y}[k]$ as

$$\mathbf{y}[k] = \mathbf{H}[k]\mathbf{x}[k] + \mathbf{n}[k]. \quad (7)$$

To transform (4b) also from complex to real, we define $\mathcal{M}(\cdot)$ to be the mapping from bit vector \mathbf{b} of length N to $\{\mathbf{x}[1], \mathbf{x}[2], \dots, \mathbf{x}[K_0]\}$ where $\mathbf{x}[k], 1 \leq k \leq K_0$ is the set of real transmission symbols defined in (5).

We can reformulate our problem into a linear programming problem with two sets of generalized vector inequalities by introducing slack variables $e_{i,k} \geq 0, 1 \leq i \leq m, 1 \leq k \leq K_0$. We also define $\mathbf{e}[k]$ to be a vector of these slack variables, i.e. $\mathbf{e}[k] = [e_{k,1}, \dots, e_{k,m}]$. Consequently we can modify the optimization problem of (4) to

$$\begin{aligned} \min \quad & \sum_{k=1}^{K_0} \sum_{i=1}^m e_{i,k} \\ \text{s.t.} \quad & \mathbf{H}[k]\mathbf{x}[k] - \mathbf{e}[k] \preceq \mathbf{y}[k] \\ & -\mathbf{H}[k]\mathbf{x}[k] - \mathbf{e}[k] \preceq -\mathbf{y}[k] \\ & \mathcal{M}(\mathbf{b}) = \{\mathbf{x}[1], \mathbf{x}[2], \dots, \mathbf{x}[K_0]\} \\ & \mathbf{b} \in \mathcal{F} \end{aligned} \quad (8)$$

Note that $x \preceq y$ denotes element-wise inequality $x_i \leq y_i$.

B. Receiver Integration of Polar Coding Constraints

Now we describe how to integrate information from the $\mathbf{b} \in \mathcal{F}$ codeword constraint into the linear programming optimization of (8) when polar codes are adopted as FEC. Feldman et al. [33] proposed one way to translate linear coding constraints from the Galois field into certain linear inequality constraints in Euclidean field. The basic idea is to relax the constraints imposed by the parity check matrix of a linear block code to define some linear codeword constraints known as fundamental polytope \tilde{Q} . Since the number of transformed linear constraints grow exponentially with the weight of the binary parity check matrix, this polytope conversion works well for those low density parity check (LDPC) codes whose sparsity parity check matrices have very low weights. The integration of such code constraints with detector has been widely investigated in [34], [35] for improved performance. Unfortunately, the dense parity check matrix of polar codes not only leads to overwhelming large number of constraints for such polytope \tilde{Q} , but also exhibits poor decoding performance when applying linear programming based on such polytope [29].

Goela et. al [29] utilized the recursive structure of polar codes that leads to a sparse graph representation with $O(N \log N)$ auxiliary variables, where N is the block length. Figure 4 shows such a factor graph of a polar code with block length $N = 2^3$. Taking advantage of this factor graph, new polytope can be defined in a space of dimension $O(N \log N)$ [29]. For this reason, we shall exploit this new polytope to generate a different set of linear coding constraints that can be incorporated into the LP receiver of (8).

Let us denote corresponding polytope as \mathcal{P} . The graph of Figure 4 shows how a polar codeword \mathbf{b} can be constructed from binary vector \mathbf{u} by a 1-1 mapping through the generator matrix \mathbf{G}_N , $\mathbf{b} = \mathbf{u}\mathbf{G}_N$. The circle nodes on the graph represent a total of $N(1 + \log N)$ binary variables and the square nodes represent the check nodes. If all the check nodes are satisfied, then \mathbf{b} is a valid codeword.

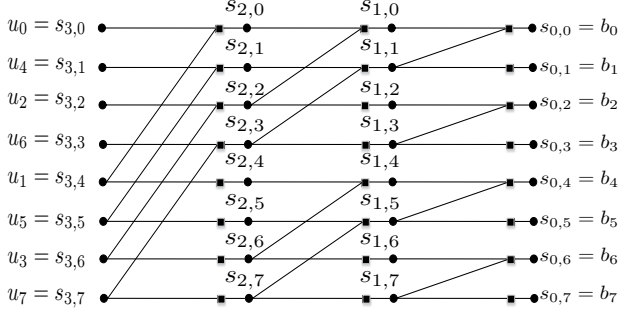


Fig. 4. factor graph representation of a polar code with block length $N = 2^3$

An example of a check node constraint in Figure 4 is

$$u_0 \oplus u_1 \oplus s_{2,0} = 0$$

where \oplus denotes modulo-2 addition. To define the relaxed polytope \mathcal{P} , we let the variables in the graph be real variables instead of binary. Note that each constraint involves only either 3 or 2 variables. Therefore, for each check node $j \in \mathcal{J}$ with 3 neighbors $\mathcal{N}(j) = \{a_1, a_2, a_3\}$, the local minimal convex polytope of check node j is \mathcal{P}_j , which can be very simply defined by below linear inequalities

$$\begin{aligned} 0 &\leq a_1 \leq a_2 + a_3, \\ 0 &\leq a_2 \leq a_3 + a_1, \\ 0 &\leq a_3 \leq a_1 + a_2, \\ a_1 + a_2 + a_3 &\leq 2 \end{aligned} \quad (9)$$

For each check node $j \in \mathcal{J}$ with only two neighbors $\mathcal{N}(j) = \{a_1, a_2\}$, the local polytope \mathcal{P}_j is defined by

$$\begin{aligned} a_1 &= a_2 \\ 0 &\leq a_1 \leq 1 \\ 0 &\leq a_2 \leq 1 \end{aligned} \quad (10)$$

Moreover, we denote the cutting plane \mathcal{T} as defined by setting all frozen variables with indices belonging to \mathcal{I}^c to zero. In summary, the polytope \mathcal{P} is the intersection of all local polytopes plus the cutting plane \mathcal{T} via

$$\mathcal{P} = \left(\bigcap_j \mathcal{P}_j \right) \cap \mathcal{T} \quad (11)$$

Therefore, we can write down the linear coding constraints by enforcing all the variables of the factor graph to comply with the polytope \mathcal{P} , i.e. $\mathbf{s} \in \mathcal{P}$ where \mathbf{s} denotes all the variables of the factor graph. These constraints can be incor-

porated into (8) as relaxed version of (4c). Therefore, the final formulation for the LP receiver can be simply written as

$$\min \sum_{k=1}^{K_0} \sum_{i=1}^m e_{i,k} \quad (12a)$$

$$\text{s.t.} \quad \mathbf{H}[k]\mathbf{x}[k] - \mathbf{e}[k] \preceq \mathbf{y}[k], \quad k = 1, \dots, K_0 \quad (12b)$$

$$-\mathbf{H}[k]\mathbf{x}[k] - \mathbf{e}[k] \preceq -\mathbf{y}[k], \quad k = 1, \dots, K_0 \quad (12c)$$

$$\mathcal{M}(\mathbf{b}) = \{\mathbf{x}[1], \mathbf{x}[2], \dots, \mathbf{x}[K_0]\} \quad (12d)$$

$$\mathbf{s} \in \mathcal{P} \subseteq [0, 1]^{N(1+\log N)} \quad (12e)$$

Note that all $N(1 + \log N)$ variables in \mathbf{s} are optimization variables in the problem of (12). As a result, the detector generates an estimate for each of these variables including \mathbf{b} . We denote the estimated bit vector as $\hat{\mathbf{b}} = [\hat{b}_1 \hat{b}_2 \dots \hat{b}_N]$. Each element $0 \leq \hat{b}_i \leq 1$ can be used to derive the likelihood of b_i to be 0 or 1. Once the log-likelihood ratio is generated by our joint LP detector, a soft-input decoder such as SC or SCL can be used to further decode $\hat{\mathbf{b}}$ to produce a final output $\hat{\mathbf{u}}$ which are the receiver outputs of the uncoded source bits. This process describes the joint detection and decoding algorithm executed by our proposed LP receiver.

IV. BLIND DETECTION SCHEME

A. PDCCH Candidates and Fractional Metric

In the system diagram shown in Figure 3, C PDCCH candidates are possibly received at the joint LP detector at the same time. The goal for the detector is first to estimate the bit sequence from the detected complex symbols reliably. For each decoded codeword which is a candidate PDCCH for the UE, the UE shall check its CRC after unmasking by its RNTI. Based on the CRC checking result, the UE determines whether or not the decoder output is a relevant DCI for the UE. The more candidates the detector pass to the decoder for decoding and CRC-checking, the higher the receiver complexity.

To reduce the receiver complexity, latency, and power consumption, it is important for the receiver to eliminate as many false candidates as possible before passing them to the decoding stage. However, it is important to note that the penalty of eliminating a correct candidate is much more severe than the benefit of rejecting a false candidate, since by missing the DCI, a UE would lose its ability to obtain its data payload in PDSCH that is destined to the UE. Such loss of DCI due to the failure of finding the right PDCCH will have a severe impact on the overall system throughput. Thus, we must take this effect into account when designing our proposed low complexity receiver algorithm that reject the false PDCCH candidates.

Note that because of RNTI unmasking, DCI for other UEs would appear to be a random bit block to the receiving UE because the unmasking RNTI would be different from the RNTI that is used to mask the DCI by the gNB transmitter. In order to help UE distinguish good PDCCH candidates from unlikely candidates, we propose a new metric that takes smaller values if the received block is a valid polar code block against the case when the received bit sequence block appears to be random bits.

Let $\mathbf{s}^* = [\mathbf{s}_1^*, \dots, \mathbf{s}_{N(1+\log N)}^*]$, $0 \leq \mathbf{s}_i^* \leq 1$ denote the solution sequence of the LP detector for the whole factor graph as defined by (12). We define a metric f

$$f = \|\mathbf{s}^* - [\mathbf{s}^*]\|_1 \quad (13)$$

The feature metric f indicates the l_1 distance between the LP solution \mathbf{s}^* and the closest vertex in the $N(1+\log N)$ -hypercube $[0, 1]^{N(1+\log N)}$. Therefore, conceptually, f is a measure of how *fractional* the LP solution is, denoting the dominance of fractional solution as discussed in [33]. We know that $\mathbf{s}^* \in \mathcal{P} \subseteq [0, 1]^{N(1+\log N)}$; however, the transmitted bit sequence in downlink corresponds to a vertex of the hypercube. Therefore, without relaxing the bit variables to $[0, 1]$, \mathbf{s}^* must be on a vertex and, consequently, f would have been zero. The closer the LP solution is to a vertex of the hypercube, the more reliable the solution is.

If the bit sequence transmitted through the channel is a valid polar codeword, and also if the SNR is high and channel state information is perfectly known, then the detector will be able to retrieve the true bit sequence from the BS transmitter. The bit sequence that was actually sent can both minimize the objective function of (4a) and also satisfy the polar code constraints simultaneously, i.e. $\mathbf{s}^* \in \mathcal{P}$. Since \mathbf{s}^* in this case would only consist of binaries integers, f would be zero as well. For larger channel noise increases, channel estimation would suffer. Thus, the LP solution would differ from the actual bits sent and therefore, the LP solution is likely to be dislodged from the vertex of the hypercube toward a fractional solution. However, under moderate to high SNR, the LP solution is still expected to be near the transmitted bit sequence. Hence, its distance from a hypercube vertex and consequently, its fractional metric f should be small and near zero.

On the other hand, consider the scenario that the DCI for a different UE is being examined as a PDCCH candidate. With the RNTI mismatch between masking and unmasking, a random bit sequence is being generated as the output by the detector as opposed to a valid polar codeword. In this case, although the correctly detected bit sequence can actually minimize the objective function of the MIMO detection at high SNR, this sequence cannot satisfy the polar code constraints of LP detector for this particular UE whose RNTI differs from the masking RNTI used by the transmitter. Hence, the transmitted sequence does not belong to the polytope \mathcal{P} . The LP detector has to find a solution that minimizes the objective function while remaining in the feasible set of (12). Therefore, the LP detector solution \mathbf{s}^* would not be necessarily close to one of the vertexes of the hypercube and can lie anywhere within the feasible set. Therefore, the metric f in this case is unlikely to be small.

To demonstrate the comparative values of f for the two cases discussed above, we present the empirical probability density functions of f under different channel conditions quantified by different levels of SNR. Let \mathcal{H}_1 denote the event that a valid polar code was transmitted sent and received by the UE, and let \mathcal{H}_0 denote the event that a random bit block was received by the UE. Furthermore, we consider both the case of perfect channel estimate and imperfect channel estimate at the

receiver. Specifically, to model imperfect channel estimates, our estimate of the channel matrix $\hat{\mathbf{H}}$ is assumed to be

$$\hat{\mathbf{H}} = \mathbf{H} + \mathbf{E} \quad (14)$$

where $\mathbf{H} = [h_{ij}] \in \mathbb{R}^{2m \times 2n}$ is the real transformation of the complex channel matrix $\tilde{\mathbf{H}}$, based on (6). Therefore, $\mathbf{H} = [h_{ij}] \in \mathbb{R}^{2m \times 2n}$ consists of i.i.d. elements such that $h_{i,j} \sim \mathcal{N}(0, 1)$. The estimation error matrix $\mathbf{E} = [e_{ij}] \in \mathbb{R}^{2m \times 2n}$ also consists of i.i.d. random elements such that $e_{i,j} \sim \mathcal{N}(0, \alpha \frac{\sigma_n^2}{2})$, where σ_n^2 is the noise variance and $\alpha \geq 1$ depends on whether there are enough pilot symbols to estimate the channel accurately or not. In our simulations we investigate two cases of $\alpha = 1$ (enough pilot symbols) and $\alpha = 2$ (short pilot length leading to estimation error variance to be double the noise variance).

As shown in Figures 5, the conditional distributions $P(f|\mathcal{H}_0)$ and $P(f|\mathcal{H}_1)$ are fully distinguishable from each other. In particular, f under \mathcal{H}_1 tends to be generally smaller whereas f under \mathcal{H}_0 tends to be much larger. As expected, the separation between the two conditional probability density functions become larger for higher SNRs. Moreover, the separation becomes less pronounced under inaccurate channel estimation. From these numerical tests, it is clear that the metric f is an effective measure on whether a detection output sequence is a likely candidate polar codeword.

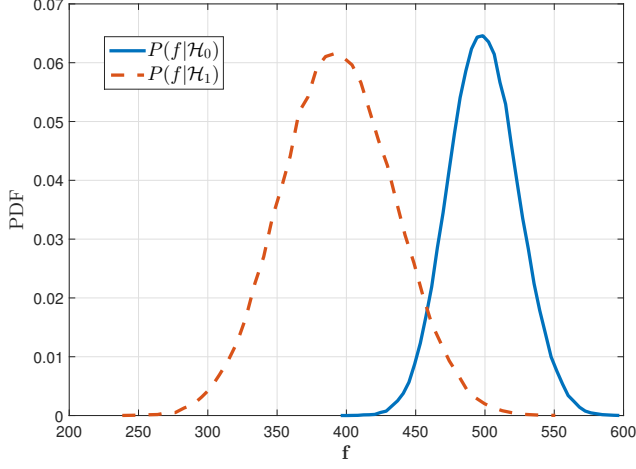
Qualitatively, $P(f|\mathcal{H}_0)$ is hardly affected by the changing SNR, since the solution under \mathcal{H}_0 can be anywhere in the feasible polytope \mathcal{P} . Thus, for event \mathcal{H}_0 , the SNR would not change how far the solution would lie from a vertex of the hypercube. On the other hand, under \mathcal{H}_1 , the detector at higher SNR becomes more successful in correctly estimating the true codeword, thereby leading to smaller values of f . For similar reason, higher SNR is needed in case of imperfect channel for the metric f to become smaller.

Figure 5 is a clear indication that the *fractional metric* f can be used to differentiate between the two cases at moderate to high SNR. We shall take advantage of f to eliminate false candidates and consequently reduce significantly the number of candidates before invoking SC/SCL decoder.

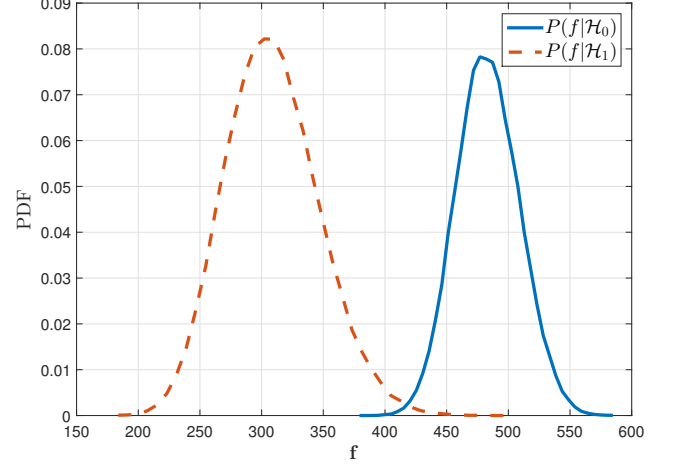
B. Effective PDCCH Candidate Trimming

Due to the large number of PDCCH candidates generated by the UE detector, we need an effective algorithm to eliminate those least likely candidates in order to lower the receiver complexity and power consumption. For each PDCCH candidate generated by the joint LP receiver, we can efficiently compute its corresponding fractional metric f . Considering the fractional metric, we propose to view the problem of candidate selection as a clustering problem in which we attempt to decide whether all C candidates are derived from probability distribution function $P(f|\mathcal{H}_0)$ or there exists one candidate in C is derived from $P(f|\mathcal{H}_1)$.

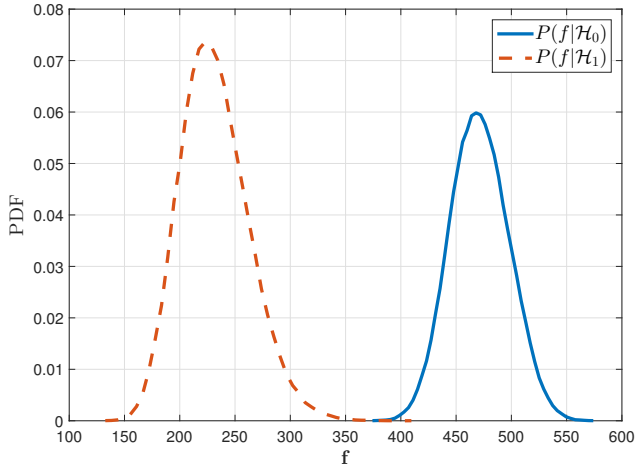
If we can determine with high probability that one candidate is likely drawn from $P(f|\mathcal{H}_1)$, then we can pass the candidate codeword to the decoder and eliminate all other $C - 1$ candidates. If we cannot have high confidence to select the most likely candidate, then we should pass a subset of C_1



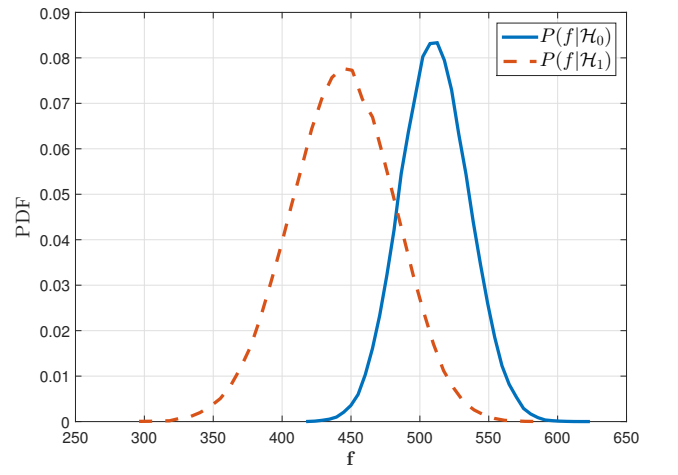
(a) SNR = 2dB, accurate channel



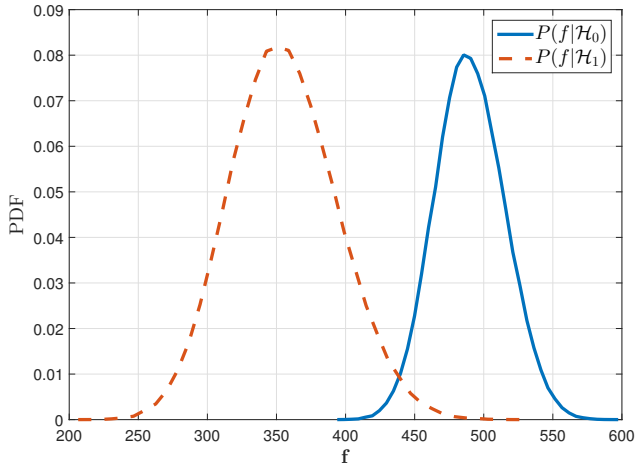
(b) SNR = 5dB, accurate channel



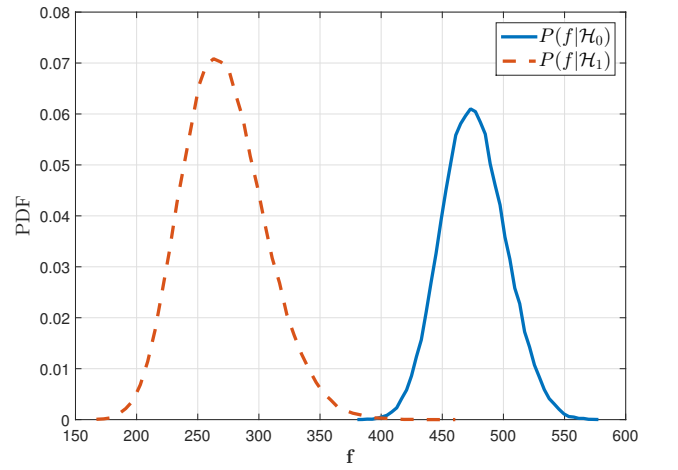
(c) SNR = 8dB, accurate channel



(d) SNR = 5dB, inaccurate channel



(e) SNR = 8dB, inaccurate channel



(f) SNR = 11dB, inaccurate channel

Fig. 5. probability density function of f under \mathcal{H}_0 and \mathcal{H}_1 for different SNRs when channel matrix is accurate/inaccurate

likely candidates from C candidates to the decoder and let CRC indicate which one is corresponding to the UE.

Let us denote $\mathbf{a} = [f_1, \dots, f_C]$ as the array that contain the fractional metrics for the C candidates. We propose the following algorithm to decide which PDCCH candidates should be passed to the decoder.

```

 $f_{\min} \leftarrow$  minimum of  $\mathbf{a}$ 
 $\tilde{\mathbf{a}} \leftarrow$  eliminate  $f_{\min}$  from  $\mathbf{a}$ 
 $\sigma \leftarrow$  standard deviation of  $\tilde{\mathbf{a}}$ 
 $\mu \leftarrow$  mean of  $\tilde{\mathbf{a}}$ 
if  $f_{\min} \leq \mu - \beta \times \sigma$  then
    send the candidate corresponding to  $f_{\min}$  to the decoder

    eliminate all other candidates
else
    send all  $C$  candidates to the decoder
end if

```

The algorithm would generate a wrong candidate only if, first of all, $P(f|\mathcal{H}_0)$ produces an f metric that deviates from its mean by $\beta \times \sigma$, where σ is the empirical standard deviation of $P(f|\mathcal{H}_0)$. Moreover, this f value must be smaller than what is drawn from $P(f|\mathcal{H}_1)$. As it can be seen from Figure (5), the probability of the latter decreases with increasing SNR and decreasing channel estimation error. The probability of the first event is also increasingly unlikely as we select increasingly larger β in our algorithm.

Our proposed algorithm has a design parameter β . The higher the value of β , the more conservative we are for declaring one valid polar codeword among the candidates. Therefore, probability of missed detection should be lower by selecting a larger β . On the other hand, a larger β also means a higher likelihood that detector passes all C candidates to the decoder, thereby leading to higher cost in terms of computation complexity, latency, and energy consumption. Therefore, by varying β we can trade the probability of missed detection on one hand for receiver cost reduction on the other hand.

Based on the empirical tests, we observe that the conditional PDF $P(f|\mathcal{H}_i)$ are approximately Gaussian. Thus, we can find an upper bound for the missed detection probability

$$\begin{aligned}
 P(\text{missed detection}) &= P((f_0 \leq f_1) \cap (f_0 \leq \mu - \beta\sigma)) \\
 &\leq P(f_0 \leq \mu - \beta\sigma) \\
 &= 1 - Q\left(-\frac{\mu - \beta\sigma - \mu}{\sigma}\right) = Q(\beta)
 \end{aligned} \tag{15}$$

Where f_1 is assumed to be the fractional metric of the right candidate and f_0 is the smallest fractional metric among all the false candidates, that are drawn from $P(f|\mathcal{H}_1)$ and $P(f|\mathcal{H}_0)$ respectively. Owing to the importance of receiving the correct control information DCI in order to be able to decode DL-SCH, we target a probability of missed detection below 10^{-6} . Since $Q(5) = 2.87 \times 10^{-7}$, $\beta \geq 5$ would be a reasonable choice. We will show that this requirement will meet our expectations in our simulation results.

V. SIMULATION RESULTS

We first present a set of simulation tests and results to demonstrate the performance of the proposed joint LP receiver in terms of bit error rate (BER) and block error rate (BLER). In particular, we will compare the joint LP receiver with a conventional decoupled MMSE detector in which detection and decoding are performed sequentially. Moreover, we will test our proposed algorithm in IV-B to demonstrate its capability to correctly identify the right PDCCH candidate for the UE. Throughout this section, we utilized the MOSEK solver [36] to solve the LP in our simulations.

A. BER and BLER

In our simulation tests, we adopt both a 4×4 spatial multiplexing MIMO model and a 4×1 transmit diversity MIMO wireless model with QPSK modulated PDCCH over a flat Rayleigh fading channel. For PDCCH, we adopt a polar code of rate = 0.5 with length $N = 128$. At the receiver, the flat fading MIMO channel is estimated for each subcarrier that also includes channel estimation errors as characterized in (14). We calculate the BER and BLER for both the decoder output and the output of the detector by hard slicing the soft information of its output.

Figure 6 shows the BER and BLER of the proposed JLP receiver with the benchmark MMSE receiver for code length of $N = 128$. Three different parameter settings are considered, respectively. The first set of results compares the JLP detector without SCL decoding against the MMSE detector without SCL decoding. It can be clearly seen from Fig. 6 that our proposed JLP receiver substantially outperforms the MMSE detector by integrating the FEC codeword constraint information during detection. Thus, this detector output that incorporates the polar code constraints can further improve the BER by as much as 12dB in terms of signal-to-noise ratio (SNR) at the BER of 10^{-3} . We further compare the effect of SCL decoding after detection output based on JLP against MMSE detection. It is clear from Fig. 6 that both BLER and BER are substantially reduced when ensuing polar decoding is adopted. In terms of BLER, the performance improvement by the JLP over MMSE can be as high as 10dB for both SCL based on $L = 1$ and $L = 4$.

Fig. 7 illustrates the performance comparison when channel estimation error variance is quite substantial, at twice the channel white noise variance, i.e. $\alpha = 2$. In this case the performance gain of JLP over MMSE is even more pronounced. JLP together with SCL decoder outperforms MMSE with SCL decoder by nearly 16 dB at the BER level of 1.5×10^{-5} . The performance improvement in JLP is to be expected since MMSE only relies the received signals without integrating the code constraints. Thus, MMSE signal detection can be more vulnerable to channel state information (CSI) error and would have no weapon to fight against CSI errors. On the other hand, JLP takes advantage of FEC coding constraints and can be more robust against both CSI error and additive channel noise.

In Figure 8, we also test the reliability of the two detectors in case of a 4×1 transmit diversity MIMO transmission. It is obvious that the channel uncertainty becomes less of an

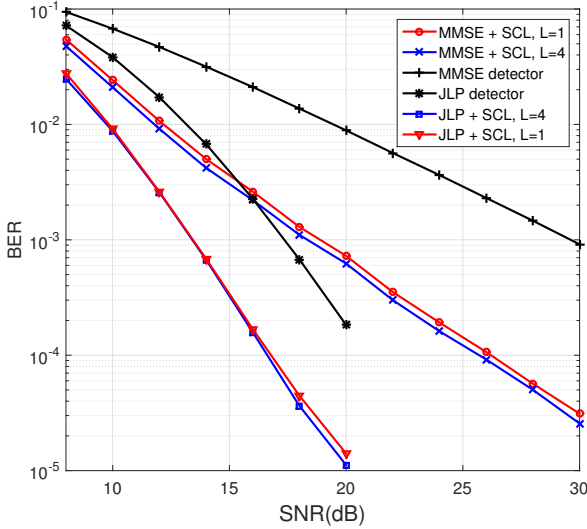
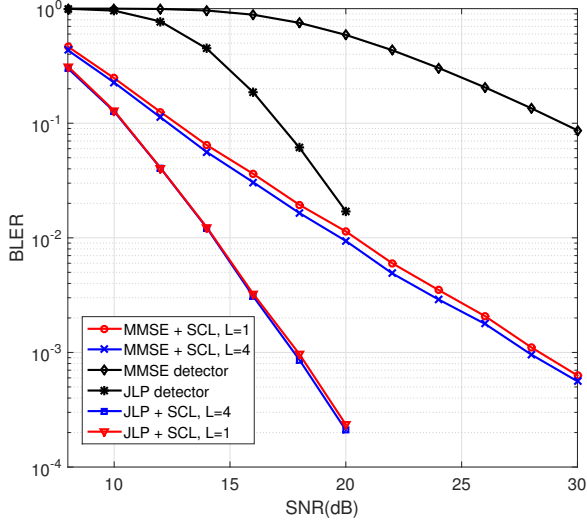


Fig. 6. Performance comparison of joint LP detector using code constraints versus decoupled MMSE, $\alpha = 1$, 4×4 MIMO

impairment than in the 4×4 case, as the 4×1 transmission diversity provides stronger resilience. Nevertheless, the JLP still outperforms the MMSE by approximately 1.5 dB, although the gap is less compared to 4×4 case.

B. Blind Detection of PDCCH

We now present the simulation results for a blind detection scenario to demonstrate the effectiveness of our proposed scheme. LP detector receives $C = 20$ PDCCH candidates with length $N = 128$ plus polar code rate of 0.5. Only one of candidates has the DCI relevant to the UE, as a result, after UE demasks its tested C candidates with its own UE-specific RNTI, at most one candidate may have the structure of a valid polar code while the remaining $C - 1$ DCI candidates would be equivalent to random blocks of bits.

We ran a Monte Carlo simulation with 10^6 trials. The channel is assumed to be a 4×1 transmit diversity MIMO channel. Both perfect and imperfect CSIs are studied. We measure

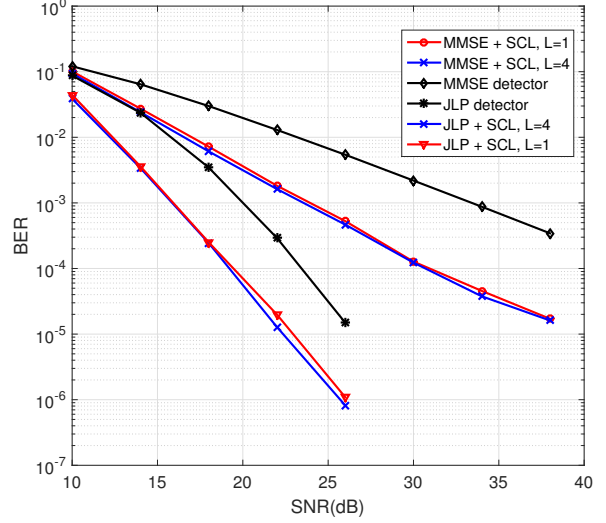
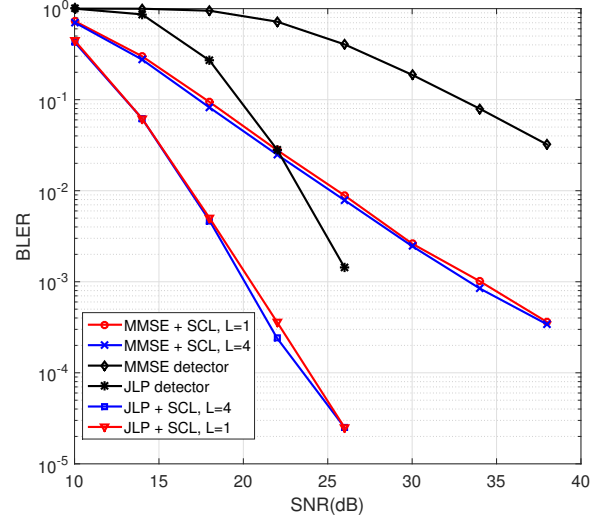


Fig. 7. Performance comparison of joint LP detector using code constraints versus decoupled MMSE, $\alpha = 2$, 4×4 MIMO

the performance of our blind detection scheme in terms of decoder usage reduction as well as the missed detection rate. Decoder usage reduction measures the ratio of instances in our simulations that our scheme is able to correctly identify the right candidate at the detector and therefore decoder usage will be only 1 instead of 20. Missed detection is defined as the probability that our blind detection scheme fails to find its own candidate and, therefore, the decoder fails to decode the right DCI, leading to lost payload.

In Table II and Table III, it is clear that our newly proposed PDCCH blind detector leads to substantial saving of decoder usage at various values of SNR and β for both perfect and imperfect CSI, respectively.

Recall that loss of DCI will cause the loss of DL-SCH payload. As a result, the gNB has to retransmit the DCI and DL-SCH again. Thus, missed detection of DCI would severely increase latency and deduce the throughput of the wireless system. Therefore, we need to set β such that missed detection

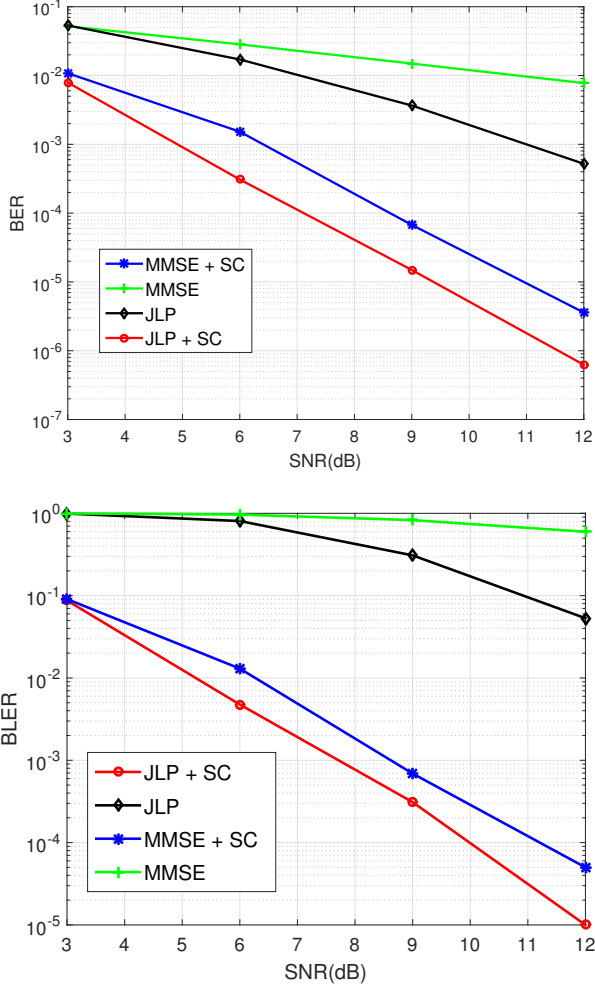


Fig. 8. Performance comparison of joint LP detector using code constraints versus decoupled MMSE, $\alpha = 1$, 4×1 MIMO

TABLE II
DECODER USAGE REDUCTION FOR PERFECT CHANNEL ESTIMATION

SNR	β	missed detection	decoder usage reduction
3	4	3×10^{-5}	51.56%
3	4.5	8×10^{-6}	38.00%
3	5	2×10^{-6}	26.10%
3	5.5	0	16.83%
5	4	3×10^{-6}	78.80%
5	4.5	0	66.62%
5	5	0	52.26%
8	4	0	97.51%
8	4.5	0	93.70%
8	5	0	86.42%

TABLE III
DECODER USAGE REDUCTION FOR IMPERFECT CHANNEL ESTIMATION

SNR	β	missed detection	decoder usage reduction
8	4	2.2×10^{-5}	56.21%
8	4.5	3×10^{-6}	41.73%
8	5	10^{-6}	28.76%
8	5.5	0	18.51%
11	4	0	90.71%
11	4.5	0	81.83%
11	5	0	69.26%

probability is as low as possible at the risk of increased decoder usage. From the results in Table II and Table III above, $\beta \geq 5.5$ leads to a missed detection probability that is low enough not to even show up in our Monte Carlo simulation of 10^6 trials. Yet, we can still benefit from the significant decoder usage reduction in moderate SNR scenarios. For instance, in case of perfect CSI, when $\text{SNR} = 8$ and $\beta = 5$, our receiver can identify the right DCI candidate 86.42% of the time while only running the SCL decoder once instead of 20 times. In case of imperfect CSI, higher SNR is needed to achieve the same performance. When $\text{SNR} = 11$ and $\beta = 5$, the decoder usage reduction of 69.26% is achieved.

Our simulation results demonstrate the benefit of our new receiver architecture. Both missed detection and decoder use reduction have been substantially contained.

VI. CONCLUSION

This work considers the important and practical problem of blind detection for user DCI in PDCCH of 5G New Radio cellular systems. To jointly reduce the receiver complexity and the probability of missed detection, we proposed a robust joint detection-decoding receiver design in MIMO systems that adopt the effective polar codes for forward error correction (FEC). We incorporate relaxed polar code constraints to formulate a novel joint LP optimization problem. The proposed receiver is more robust against CSI errors, channel noises, and other non-idealities at the wireless receivers. We also introduced a metric at the LP detector that is capable of identifying the right PDCCH candidate while rejecting the false ones. The use of this metric improves the so called blind detection process in NR standard. Our proposed joint LP detector can also directly interface with well-known polar decoders such as SC and SCL decoders for effective error correction. As a result, JLP detector can be an appropriate receiver candidate to be used for control channels of 5G systems. Our test results demonstrate superior receiver performance particularly when CSI knowledge is inaccurate due to practical obstacles such as short pilot length and pilot contamination. The results further show that our proposed fractional metric can identify the right candidate in moderate to high SNR scenarios with negligible probability of missed detection.

REFERENCES

- [1] 3rd Generation Partnership Project (3GPP), "Evolved Universal Terrestrial Radio Access (E-UTRA); Radio Resource Control (RRC); Physical layer procedures," Technical Specification (TS) 36.213, 06, version 15.2.0.
- [2] 3rd Generation Partnership Project (3GPP), "Technical Specification Group Radio Access Network; NR; Physical layer procedures for control," Technical Specification (TS) 38.213, 06, version 15.2.0.
- [3] S.-L. Shieh, S.-T. Kuo, P.-N. Chen, and H. Yungshiang, "Strategies for blind transport format detection using cyclic redundancy check in UMTS WCDMA," in *Wireless And Mobile Computing, Networking And Commun., 2005.(WiMob'2005), IEEE International Conf. on*, vol. 2. IEEE, 2005, pp. 44–50.
- [4] R. Moosavi and E. G. Larsson, "A fast scheme for blind identification of channel codes," in *Global Telecommun. Conf. (GLOBECOM 2011), 2011 IEEE*. IEEE, 2011, pp. 1–5.
- [5] T. Sipila, "Blind transport format detection based on decoder metric," Oct. 9 2012, uS Patent 8,286,058.

- [6] D. P. Malladi, J. Montojo, and S. Sarkar, "Methods and systems for PDCCH blind decoding in mobile communications," Aug. 7 2012, uS Patent 8,238,475.
- [7] T. Xia and H.-C. Wu, "Novel blind identification of LDPC codes using average LLR of syndrome a posteriori probability," *IEEE Trans. Signal Process.*, vol. 62, no. 3, pp. 632–640, 2014.
- [8] J. Zhou, Z. Huang, C. Liu, S. Su, and Y. Zhang, "Information-dispersion-entropy-based blind recognition of binary BCH codes in soft decision situations," *Entropy*, vol. 15, no. 5, pp. 1705–1725, 2013.
- [9] E. Arıkan, "Channel polarization: A method for constructing capacity-achieving codes for symmetric binary-input memoryless channels," *IEEE Trans. Inf. Theory*, vol. 55, no. 7, pp. 3051–3073, 2009.
- [10] E. Arıkan, "A performance comparison of polar codes and Reed-Muller codes," *IEEE Commun. Lett.*, vol. 12, no. 6, 2008.
- [11] I. Tal and A. Vardy, "How to construct polar codes," *IEEE Trans. Inf. Theory*, vol. 59, no. 10, pp. 6562–6582, 2013.
- [12] D. Wu, Y. Li, and Y. Sun, "Construction and block error rate analysis of polar codes over awgn channel based on gaussian approximation," *IEEE Commun. Lett.*, vol. 18, no. 7, pp. 1099–1102, 2014.
- [13] A. Bravo-Santos, "Polar codes for the Rayleigh fading channel," *IEEE Commun. Lett.*, vol. 17, no. 12, pp. 2352–2355, 2013.
- [14] I. Tal and A. Vardy, "List decoding of polar codes," in *ISIT*, 2011, pp. 1–5.
- [15] E. Viterbo and J. Boutros, "A universal lattice code decoder for fading channels," *IEEE Trans. Inf. theory*, vol. 45, no. 5, pp. 1639–1642, 1999.
- [16] P. W. Wolniansky, G. J. Foschini, G. Golden, and R. A. Valenzuela, "V-BLAST: An architecture for realizing very high data rates over the rich-scattering wireless channel," in *Signals, Syst., and Electronics, 1998. ISSSE 98. 1998 URSI Int. Symp.* IEEE, 1998, pp. 295–300.
- [17] C. Douillard, M. Jézéquel, C. Berrou, D. Electronique, A. Picart, P. Didier, and A. Glavieux, "Iterative correction of intersymbol interference: Turbo-equalization," *European trans. on telecommun.*, vol. 6, no. 5, pp. 507–511, 1995.
- [18] B. Lu, X. Wang, and K. R. Narayanan, "LDPC-based space-time coded OFDM systems over correlated fading channels: Performance analysis and receiver design," *IEEE Trans. Commun.*, vol. 50, no. 1, pp. 74–88, 2002.
- [19] B. M. Hochwald and S. Ten Brink, "Achieving near-capacity on a multiple-antenna channel," *IEEE Trans. Commun.*, vol. 51, no. 3, pp. 389–399, 2003.
- [20] K. Wang and Z. Ding, "Joint turbo receiver for LDPC-coded MIMO systems based on semi-definite relaxation," *arXiv preprint arXiv:1803.05844*, 2018.
- [21] K. Wang and Z. Ding, "Integrated semi-definite relaxation receiver for LDPC-coded MIMO systems," *arXiv preprint arXiv:1806.04295*, 2018.
- [22] K. Wang, H. Shen, W. Wu, and Z. Ding, "Joint detection and decoding in LDPC-based space-time coded MIMO-OFDM systems via linear programming," *IEEE Trans. Signal Process.*, vol. 63, no. 13, pp. 3411–3424, Apr. 2015.
- [23] K. Wang, W. Wu, and Z. Ding, "Joint detection and decoding of LDPC coded distributed space-time signaling in wireless relay networks via linear programming," in *Proc. IEEE Int. Conf. Acoust., Speech, Signal Process. (ICASSP), Florence, Italy*, July 2014, pp. 1925–1929.
- [24] K. Wang and Z. Ding, "Robust receiver design based on FEC code diversity in pilot-contaminated multi-user massive MIMO systems," in *IEEE Int. Conf. on Acoust., Speech and Signal Process. (ICASSP), Shanghai, China*, May 2016.
- [25] K. Wang and Z. Ding, "FEC code anchored robust design of massive MIMO receivers," *IEEE Trans. Wireless Commun.*, vol. 15, no. 12, pp. 8223–8235, Sept. 2016.
- [26] K. Wang, W. Wu, and Z. Ding, "Diversity combining in wireless relay networks with partial channel state information," in *IEEE Int. Conf. on Acoust., Speech and Signal Process. (ICASSP), South Brisbane, Queensland*, Aug. 2015, pp. 3138–3142.
- [27] K. Wang and Z. Ding, "Diversity integration in hybrid-ARQ with Chase combining under partial CSI," *IEEE Trans. Commun.*, vol. 64, no. 6, pp. 2647–2659, Apr. 2016.
- [28] A. Jalali and Z. Ding, "A joint detection and decoding receiver design for polar coded mimo wireless transmissions," in *IEEE Int. Symp. Inf. Theory (ISIT)*. IEEE, 2018, pp. 1011–1015.
- [29] N. Goela, S. B. Korada, and M. Gastpar, "On LP decoding of polar codes," in *Inform. Theory Workshop (ITW), 2010 IEEE*. IEEE, 2010, pp. 1–5.
- [30] C. Condo, S. A. Hashemi, and W. J. Gross, "Blind detection with polar codes," *IEEE Commun. Lett.*, vol. 21, no. 12, pp. 2550–2553, 2017.
- [31] P. Giard, A. Balatsoukas-Stimming, and A. Burg, "Blind detection of polar codes," *arXiv preprint arXiv:1705.02111*, 2017.
- [32] T. Cui, T. Ho, and C. Tellambura, "Linear programming detection and decoding for MIMO systems," in *Inform. Theory, 2006 IEEE Int. Symp.* IEEE, 2006, pp. 1783–1787.
- [33] J. Feldman, M. J. Wainwright, and D. R. Karger, "Using linear programming to decode binary linear codes," *IEEE Trans. Inf. Theory*, vol. 51, no. 3, pp. 954–972, 2005.
- [34] K. Wang, "Galois meets Euclid: FEC code anchored robust design of wireless communication receivers," Ph.D. dissertation, University of California, Davis, 2017.
- [35] K. Wang, "Semidefinite relaxation based blind equalization using constant modulus criterion," *arXiv preprint arXiv:1808.07232*, 2018.
- [36] E. Andersen and K. Andersen, "The MOSEK optimization toolbox for MATLAB manual. version 7.0, 2013."